doi:10.1017/S1431927617008546
Microsc. Microanal. 23 (Suppl 1), 2017

Dissecting Electronic Structure of a New Line Defect in $NdTiO_3$ by EELS

K. Andre Mkhoyan

Department of Chemical Engineering and Materials Science, University of Minnesota, Minneapolis, MN, USA

Perovskite oxides are one of the most abundant natural materials on the Earth. The flexibility of the perovskite structure allows to accommodate cations of different sizes and valences. Wide variety of properties have been demonstrated in bulk perovskites, at their interfaces, or heterostructures made from them including room-temperature ferroelectricity [1], giant piezoelectricity [2], quantum oscillation [3], two-dimensional superconductivity [4], and many more. The elemental diversity, stability even under off-stoichiometry conditions, and variety of crystal symmetries in the perovskite structure make it a natural host for a range of defects as well. While several point and planar defects have been reported in perovskites [5,6] with some of them quite unique for perovskites, no new line defect, other than standard dislocations, has been observed until recently (Figure 1) [7].

We characterize this new line defect, observed in perovskite $NdTiO_3$ (NTO) films, using a combination of high-resolution analytical scanning transmission electron microscopy (STEM) imaging, atomic-scale energy dispersive X-ray spectroscopy (EDX) and electron energy-loss spectroscopy (EELS), and *ab initio* calculations. Two high-angle annular dark-field (HAADF) STEM images of such NTO films with and without this new line defect are shown in Figs. 1a, b.

The result of detailed EELS analysis of the defect core is presented in Figure 2. EELS data recorded across the core of the defect indicates distinct changes in its fine structure. Ti $L_{2,3}$ spectra show that Ti^{3+} character changes to predominantly Ti^{4+} when the probe moves from the bulk to the core of the defect. The transition is not abrupt and occurs over a distance of 1 nm from the defect center. O *K* EELS spectra also show changes in the fine structure across the defect. When compared with DFT+U calculations, these changes are in quantitative agreement in terms of the edge onset, onset peak height, and width of the second peak at 535-540 eV (Figure 2 d,e). The results indicate that the main differences between electronic states of Ti and O atoms occur at the boundary between defect and the bulk, and not at the core. These results also indicate that the *ab initio* structural determination is quite reliable and the electronic structure of the line defect is indeed considerably different from that of bulk NTO [8].

References:

[1] J. H. Haeni *et al.,* Nature **430**, (2004), p. 758.
[2] S. H. Baek *et al.,* Science **334**, (2011), p. 958.
[3] Y. Kozuka *et al.,* Nature **462**, (2009), p. 487.
[4] N. Reyren *et al.,* Science **317** (2007), p. 1196.
[5] D. J. Keeble *et al.,* Phys. Rev. Lett. **105** (2010), p. 226102.
[6] S. Farokhipoor *et al.,* Nature **515** (2014), p. 379.
[7] J. S. Jeong *et al.,* Nano Lett. **16** (2016), p. 6816.
[8] This work was supported in part by NSF DMR-0819885 and DMR-1420013, also in part by NSF DMR-1410888, NSF EAR-134866 and EAR-1319361.

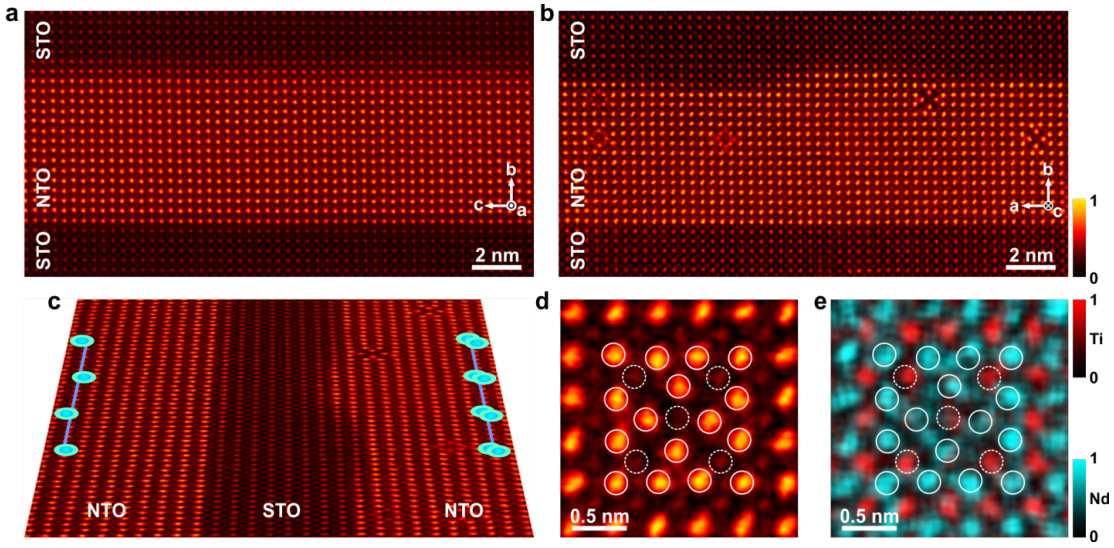

Figure 1. a, HAADF-STEM image of an NTO film viewed along the *a*-axis. **b,** Another NTO film viewed along the *c*-axis showing several line defects. **c,** An inclined HAADF image including both films along the *a*- and *c*-axis, is presented to show the arrangement of Nd columns in the NTO films. A magnified HAADF-STEM image (**d**) is shown along with a STEM-EDX spectrum-image (**e**) of a line defect composed by Nd *L* (cyan) and Ti *L* (red) signals. Positions of Nd columns, which moved into Ti/O vacant columns, are indicated with the dashed circles (modified from Ref. [7]).

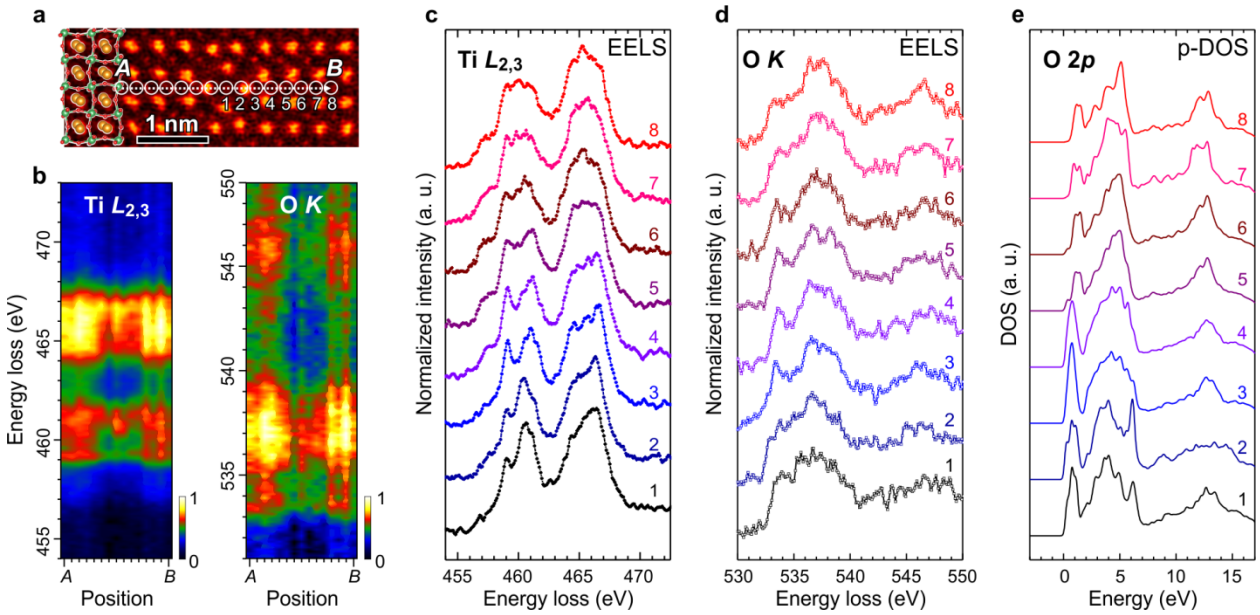

Figure 2. a, ADF-STEM image of a line defect showing the positions of EELS line profile (from *A* to *B*). **b,** EELS Ti $L_{2,3}$ (left panel) and O *K* (right panel) spectra vs. position. **c-d**. The fine structure of the Ti $L_{2,3}$ and O *K* measured across the defect. **e,** (DFT+U)-calculated O 2*p* p-DOS at each position. Gaussian broadening with FWHM of 0.3 eV was applied to calculated p-DOS. Probe positions (1-8) correspond to those labeled in **a** (modified from Ref. [7]).

https://doi.org/10.1017/S1431927617008546 Published online by Cambridge University Press